Synchrotron-aided reconstruction of the conodont feeding apparatus and implications for the mouth of the first vertebrates

Nicolas Goudemand[a,1], Michael J. Orchard[b], Séverine Urdy[a], Hugo Bucher[a], and Paul Tafforeau[c]

[a]Palaeontological Institute and Museum, University of Zurich, CH-8006 Zürich, Switzerland; [b]Geological Survey of Canada, Vancouver, BC, Canada V6B 5J3; and [c]European Synchrotron Radiation Facility, 38043 Grenoble Cedex, France

The origin of jaws remains largely an enigma that is best addressed by studying fossil and living jawless vertebrates. Conodonts were eel-shaped jawless animals, whose vertebrate affinity is still disputed. The geometrical analysis of exceptional three-dimensionally preserved clusters of oro-pharyngeal elements of the Early Triassic *Novispathodus*, imaged using propagation phase-contrast X-ray synchrotron microtomography, suggests the presence of a pulley-shaped lingual cartilage similar to that of extant cyclostomes within the feeding apparatus of euconodonts ("true" conodonts). This would lend strong support to their interpretation as vertebrates and demonstrates that the presence of such cartilage is a plesiomorphic condition of crown vertebrates.

apical cartilage | conodont oral skeleton | early vertebrates | homology

How the transition from "agnathans" to gnathostomes ("jawed" vertebrates) occurred is one of the most intriguing problems of evolutionary biology (1). Little is known about the endoskeleton of fossil jawless vertebrates [e.g., fossil cyclostomes (hagfishes and lampreys) and "ostracoderms"]. Although the view is still debated (2), euconodonts would have possessed the very first vertebrate mineralized skeleton in the form of their oral denticles (3, 4).

The general architecture of the conodont oral skeleton is a bilaterally symmetrical array of usually 15 phosphatic elements, which generally becomes disarticulated after the decay of the supporting tissues. Hence most conodonts are known only as isolated elements. From the detailed study of hundreds of articulated "natural assemblages" and photographic simulation of their collapse, Purnell and Donoghue (5) constructed a 3D model of the *Idiognathodus* apparatus [presumably a template for all ozarkodinid apparatuses (6)] in which one pair of obliquely pointed M elements are located rostrally and, behind them, one unpaired S_0 (subscript number indicates distance ordering from the symmetry axis) element lying on the axis of bilateral symmetry and four pairs of elements (S_{1-4}) located on both sides of the S_0 would have grasped food and, more caudally, two pairs of pectiniform elements (P_1, P_2) would have processed this food by crushing and/or slicing (5, 7, 8) (Fig. 1 *A–B*) (for "standard" orientation of single elements, see Fig. S1). Purnell and Donoghue's reconstruction of a generalized resting (dead) position is very well supported and in most aspects very convincing. It is therefore adopted here as a basis upon which we build our dynamic reconstruction of the feeding apparatus at work.

How could these elements actually grasp or cut prey tissues? Purnell and Donoghue's functional model (section 6 of ref. 5) was based chiefly on analogies with extant agnathans. Indeed, the "quite simple" geometry of the *Idiognathodus* elements does not provide much indication of what motions are possible or not [except for uncommon natural assemblages (see below)]. Thus, hypotheses were inferred from extant putative closest relatives. In our view, the more "complicated" *Novispathodus* apparatus imposes additional constraints that enable us to reconstruct the movement of the elements independently of phylogenetic con-

siderations. Despite the absence of any preserved traces of oral cartilages in the rare specimens of conodonts with partly preserved soft tissue (10), we show that partial reconstruction of the conodont mouth is possible through biomechanical analysis.

Results

We recently discovered several fused clusters (rare occurrences of exceptional preservation where several elements of the same animal were diagenetically cemented together) of the Early Triassic conodont *Novispathodus* (11). One of these specimens (Fig. 2*A*), found in lowermost Spathian rocks of the Tsoteng section (Tiandong District, Guangxi Province, China) (12, 13), consists of four "grasping" elements (S_{1-4} elements).

Fused clusters partially preserve the relative 3D positions and orientations of the involved elements. However, they are very small, fragile, tricky to manipulate, and if more than two or three elements are involved, very complicated to analyze. One way to circumvent this is to use a nondestructive imaging method such as X-ray microtomography. In our case, the required resolution and contrast could not be achieved with conventional microtomography. Hence, we scanned this Chinese cluster, as well as a complete set of isolated elements (catalog nos. PIMUZ 39841–9) found in the same sample and belonging to the same multielement species, at the European Synchrotron Radiation Facility, on the ID19 beamline, using submicron resolution propagation phase-contrast X-ray synchrotron microtomography (PPC-SRμCT) (14) (*Methods*). On the basis of refs. 6, 11, and 15, we reconstructed a virtual 3D apparatus of *Novispathodus*. The relative sizes of the S_{1-4} elements were inferred from the cluster. The other relative sizes (M, S_0, P_1, P_2 relative to S_{1-4}) were derived from the few known *Neogondolella* natural assemblages (Fig. 2 *B–C*) (15, 16).

Both our *Novispathodus* cluster and the *Neogondolella* natural assemblages (15, 16) show that the cusps of the S_1 and S_2 elements were oriented more caudally than those of the S_0 and $S_{3,\,4}$ elements, a feature that Orchard and Rieber considered to be unique to the "gondolellaceans" (15, p. 480). Its recurrence in all known Triassic assemblages (17 and 18) independently of their collapse angle suggests that it is not due to a taphonomic bias (postmortem rotation of elements) and indeed records a configuration that differs from the *Idiognathodus* reconstruction (5). Natural assemblages of *Ozarkodina*, the presumed rootstock of the Ozarkodinida (19), indicate that this caudal orientation of
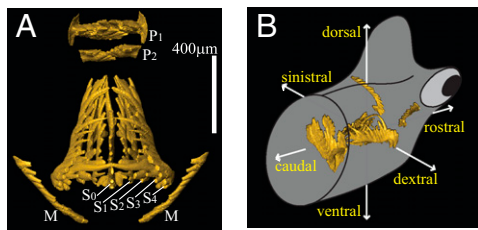
Fig. 1. Anatomical notation and orientation. (*A*) Dorsal view of the reconstructed, closed apparatus of *Novispathodus*. Anatomical notation after Purnell et al. (9). (*B*) Orientation of the apparatus within the conodont's head.

the cusp of the S_1 is not restricted to the Gondolelloideans (ref. 20, reinterpreted in ref. 6, fig. 13A; 21).

Fused clusters involving only the two hindeodelliform S_3 and S_4 elements are relatively more frequent in our collections. This suggests that they were located close and subparallel to one another (their recurrent relative position in those clusters) and had probably a common motion within the living animal. In (ab)oral view, their respective posterior processes are substraight posteriorly and outwardly deflected behind the cusp, and their anterior processes are laterally bowed inward, which results in an overall sitar-like profile.

The shape of the S_2 fits those of the S_3 and S_4 in the following aspects: (*i*) In the "cluster position" (see above) where the cusp of the S_2 is subparallel to the posterior processes of the S_3 and S_4 elements, the outer profile (oral view) of the S_2 is similar to the inner profile of the S_3, and the largest denticle of its antero-lateral process is aligned with the cusps of the S_3 and S_4 (Figs. 2*A* and 3*B*). (*ii*) In a presumed "growth position" where the respective basal cavities (initial growth centers) of the S_{2-4} elements are approximately aligned and the inner lateral process of the S_2 is parallel to the posterior processes of the S_3 and S_4 (Fig. 3*C*), the respective profiles of S_{2-4} in ventral view still match, as do their lower margins in lateral view. In this growth position (which also corresponds to the resting position of *Idiognathodus*) (5), the antero-lateral process of the S_2 extends more rostrally than the anterior processes of the S_3 and S_4 and is outwardly deflected in a way that somehow complements the rostral denticulation of the S_3 and S_4 (Fig. 3*D*, ventral view; note the alignment of the anteriormost denticles of the S_2 with the tangent of the S_4's outline at the anterior end). This indicates that, at least in gondolelloideans, the S_2 had a pivot motion relative to the S_3 and S_4 elements.
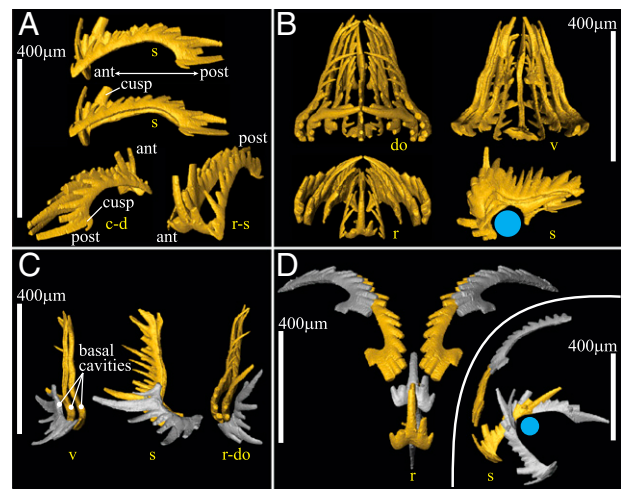
Fig. 3. Geometrical correspondences between elements. (*A*) The S_1 elements match the posterior process of the S_0. Per definition, the tip of the cusp points posteriorly. ant: anterior; post: posterior. (*B*) Closed arrangement of S elements. (*C*) Presumed growth position of the S_2 (silver) as inferred by geometrical correspondences with the S_3 and S_4 elements (gold). (*D*) Proposed movement of the S_0 against the M elements (silver: start and end positions; gold: pinching position). (*A–D*) c: caudal; d: dextral; do: dorsal; r: rostral; s: sinistral; v: ventral; blue circles: hypothetical cartilage.

If we assume that the various elements moved along trajectories approximately parallel to the curvature of the cusp and denticles (5), then the movements of the S_{2-4} elements must have included an opening/closing pivot motion around an axis parallel to the posterior processes of the S_3 and S_4. Consequently, the net motion of the S_2 element was the composition of at least two pivot motions around two nearly perpendicular axes, and hence its trajectory must have been subhelicoidal, which is compatible with the peculiar right-angled configuration of its processes. The minimal distance between sinistral and dextral sets of S_{2-4} elements is constrained by the dimensions of their respective cusps and denticles and of the inner lateral processes of both S_2 elements (broken in this specimen; Fig. 2*A*, arrow) (Fig. S1). Moreover, an efficient grasping could have been achieved only if the tips of the denticles were directed subrostrally, that is, toward the prey in an opened position (Fig. 4 *A*, *a*).

The curvature of the cusp and denticles of the S_0 element suggest both a rotation about a point located posteriorly on the
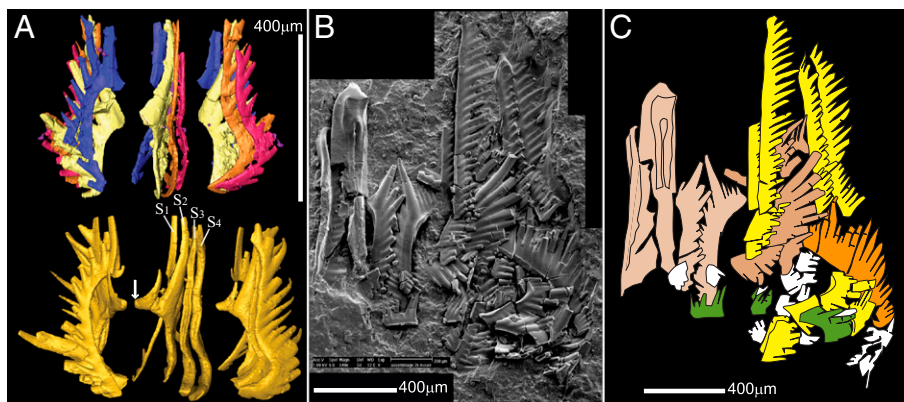
Fig. 2. Fossil material and interpretation. (*A*) Comparison of the scanned cluster specimen (*Upper*) with a partial reconstruction based on isolated elements (*Lower*). The arrow indicates a broken process. (*B*) SEM composite microphotograph and (*C*) interpretation of a natural assemblage of *Neogondolella* found by Rieber (also ref. 16) from the Middle Triassic at Monte San Giorgio, Switzerland. Beige: P elements; orange: S_0; brown: S_1 and S_2; yellow: S_3 and S_4; green: M elements.

Fig. 4. Proposed relative positions and movements of the elements in *Novispathodus* (*A*) and *Idiognathodus* (*B*). Color coding as in Fig. 2*C*; blue circles: hypothetical cartilage. (*A*, *a* and *c* and *B*, *a* and *b*) Respectively, rostral and sinistral views of the opened (protracted) apparatus. (*A*, *c* and *d*) S_3 and S_4 elements of *Novispathodus* could have closed independently in the protracted position and performed grasping before the S_0 and M elements cut the prey's tissues. (*A*, *b* and *e* and *B*, *a* and *c*) Pinching position. (*A*, *f* and *B*, *d*) Intermediate position. (*A*, *g* and *B*, *e*) Closed (retracted) position. (*B*, *f*) Original at rest reconstruction of *Idiognathodus* (compare with *B*, *d*); redrawn after Purnell and Donoghue (5). (*A* and *B*) In lateral views, only the dextral "half" of the apparatus is represented. P elements are represented only in *A*, *g* and *B*, *f*.

posterior process and an arched antero-posterior translation. Similarly, the movement of the S_1 must have included an arched antero-posterior translation accompanied by an opening/closing pivot about its main axis. Interestingly, the outline of the latter element very closely matches the outline of the posterior process of the S_0 (Fig. 3*A*), which suggests that the S_0 and the two S_1 elements grew and probably functioned together.

This position of the S_0 respective to the S_1 is compatible with the relative positions of the S_{1-4}, as recorded by our cluster. In fact, if all S elements are reconstructed in these respective positions (Fig. 3*B*), we get a very compact arrangement where all denticle tips end up close to the midplane (represented here by the length axis of the S_0 element) and the lower margins are subparallel in lateral view. We propose that this particular spatial configuration, partly recorded by our cluster, corresponds to the maximal closing position of the grasping S "module" (Fig. 4*A*, *g*).

This arrangement is rather uncommon for a natural assemblage, and it differs substantially from the "at rest" arrangement, as reconstructed by Purnell and Donoghue (5, 6). However, several published natural assemblages (for an exhaustive list of those published before 1998, see appendix in ref. 6) also record relative orientations of elements that differ significantly from Purnell and Donoghue's reconstruction (that is, in a way that is not convincingly explained by ad hoc postmortem displacements of the elements). In particular, a "very uncommon" subparallel arrangement of the S_{2-4} and M elements of *Gnathodus*, originally figured by Schmidt (22; reillustrated in ref. 6, figs. 7 and 8), or a specimen of *Bispathodus* where the converging cusps of the M elements come in contact with one another (fig. 14 and plate 3 in ref. 6). Furthermore, we consider that some of the variation observed among the numerous specimens of *Idiognathodus* natural assemblages is best explained if one assumes that they record several slightly differing "living" positions rather than one single "resting" position affected by taphonomic noise. Hence, in our view, natural assemblages are potentially informative about the relative motions of the elements.

Theoretically, the geometrical analysis of the flattening of a few pairs of bilaterally symmetrical elements is sufficient for solving the inverse mapping problem of estimating the 3D angle of collapse. The relative orientation and spacing of these pairs of

Fig. 5. Comparison with extant lamprey and other conodont taxa. (*A*) (*Left*) Supraoral tooth (green) and lingual laminae (orange: transverse lamina; yellow: longitudinal laminae) of the lamprey *G. australis*. (*Right*) Sagittal sections of the lamprey head in protracted (middle) and retracted (right) positions. Red: muscles; cyan: cartilages. Redrawn after Hilliard et al. (23). (*B*–*D*) Proposed relative positions and movements of the elements of *Ellisonia* (*B*), *Hibbardella* (*C*), and *Paracordylodus* (*D*). Isolated S_{1-4} in lower rows. Color coding as in Fig. 2*C*; light orange: basal body. Modified, respectively, after Koike et al. (24), Nicoll (25), and Tolmacheva and Purnell (26). (*B*) M is missing.

elements can then be solved independently for each (obliquely collapsed) specimen, and analysis of numerous specimens not only allows smoothing taphonomically induced discrepancies but also gives insights about the relative motions of the elements.

The integration of this information, in particular from our cluster and other uncommon assemblages, into a comprehensive, dynamic model implies a rotation of the $S_{3,4}$ elements relative to the S_0 about a medio-lateral axis approximately located below the cusp of the S_0. From the at rest position, maximal closing of the apparatus is most plausibly attained by dorso-caudal retraction of the $S_{3,4}$ toward the P elements rather than by rostral eversion of the S_0. Note that the longitudinal dimensions of the largest S elements approximately equal the distance between this presumed rotation axis and the P_2 elements and are thus compatible with this interpretation (Fig. 4 A, f and g and B, e and f).

Each euconodont element is composed of two parts: a crown and a basal body. The latter is preserved only in exceptional cases. In S or M elements, the basal body, when present, smoothes out the lower margin (ventral outline) of the element (Fig. 5 C–D). In *Novispathodus*, the lower margins of the S elements are already smooth (low 3D curvature), and we therefore assume that their respective basal bodies, if mineralized, were relatively thin and filled up the basal grooves but did not alter the shape of their lower margins substantially (Fig. S1).

If the latter assumption holds, then it is clear from Figs. 3B and 4A that a single and simple mechanism can explain all of the above deduced motions of the elements: a pulley-like system with protractor and retractor muscles that would have rotated the elements about a ventral, medio-laterally oriented, cylinder-shaped or possibly U-shaped (both slightly curved ends pointing dorso-rostrally) supporting element of unknown but most probably cartilaginous nature (Figs. 3–5, blue circle). Only three pairs of antagonistic muscles (inserted, respectively, on $S_{0,1}$, S_2, and $S_{3,4}$) would have been necessary to operate the nine S elements in the way described here.

Interestingly, this "pulley hypothesis" also possibly accounts for the presence of the two inward and forward pointing M elements: The lower profile of the *Novispathodus* S_0, especially the arched part of its posterior process, suggests that during opening it was first rostro-ventrally translated and then rotated (its arched posterior end "gliding" on the ventral cartilage), and vice versa during closure. Its dimensions are compatible with its

initial rotation being synchronized with the closure of the M elements (Figs. 3D and 4 A, e). Together, their overall Y-shaped (in rostral view) converging motion would have performed an efficient pinching and seizing function. The uncommon arrangement of *Bispathodus* illustrated by Purnell and Donoghue (plate 3 and fig. 14 in ref. 6) lends partial support to this scenario. The subsequent dorso-caudal retraction of the S_0 and S_1 elements would have torn off the tissues of prey and brought them toward the pectiniform elements. Then, the other S elements would have closed, further channelling the food toward the pharynx (Fig. 4A and Movies S1 and S2).

Discussion

Our model strongly recalls the operation of the lingual laminae of lampreys such as the flesh-feeder species *Geotria australis* (23) (Fig. 5A). In the fully protracted position, a pair of longitudinal lingual laminae can open and close independently and pinch the prey's tissues. During subsequent retraction, the interlocking of the transverse lingual lamina with the supraoral tooth cuts the flesh off, and the longitudinal laminae brings it toward the pharynx (23). The growth and phosphatic composition of the conodont elements prevent homology of the conodont elements themselves with the keratin "teeth" of extant agnathans (4, 27, *contra* ref. 28). However, our model supports the view that the oral apparatus of conodonts as a whole is homologous with the lingual apparatus of lampreys. We tentatively homologize the presumed ventral cartilage with the *cartilago apicalis* of extant lampreys (29). In lampreys, this cartilage is flexibly attached to a larger piston cartilage (23) (Fig. 5A). In *Novispathodus*, the available data do not constrain its shape caudo-ventrally, and a similar mechanism can only be hypothesized.

In our view, the S elements were not necessarily lying on dental plates (*contra* ref. 5). At least for *Novispathodus* the location of the ventral cartilage is constrained by the shape and motion of the S_2 elements, and space considerations contradict the presence of such plates. In *Novispathodus*, if cartilaginous dental plates were present, they were restricted to the posterior processes of the S_3 and S_4 and thus analogous to the paired *cartilago apicalis lateralis* of lampreys (29). By analogy with lampreys, additional muscles located between the apical lobes and the apicalis (23) would have allowed performing independent

Fig. 6. Hypothesis of relationships among chordates that is primarily based on refs. 27 and 30. Evidence from molecular data supports monophyly of cyclostomes and shows that the closest relatives of vertebrates are the tunicates, not the cephalochordates (31). The relationships among euconodonts are derived from ref. 32. Blue circles indicate the presence of a lingual cartilage.

opening/closing of these elements (analogous to the longitudinal lingual laminae) in the protracted position.

Further work is necessary to assess to what extent this reconstruction is compatible with other conodont taxa, but we consider that the presence of a ventral apical cartilage and the proposed seizing movement of the S_0 and M elements were possibly shared by most euconodonts (Fig. 5 B–D and Fig. 6). Although we consider the presence of a flexible, half-circular ventral cartilage as obvious in the Ordovician balognathid *Promissum pulchrum* [described by Aldridge et al. (33)], the closure of the S elements occurred certainly in a ventral rather than dorsal position (see uncommon arrangement in figs. 7–9 in ref. 33). Thus, the shape of the ventral cartilage and the putative pulley-like motion of the various S elements must have varied within the clade. However, if, as suggested, the presence of such cartilage is established in even the most basal forms of complex conodonts (32), such as the Early Ordovician (ca. 480 million years old) *Paracordylodus* (Fig. 5D), then it should reflect a plesiomorphic condition of euconodonts. It cannot be confirmed yet whether conodonts, whose apparatus is composed of coniform elements only, could have shared this characteristic but similarities between the apparatuses of panderodontids and euconodonts (7, p. 90) favor this hypothesis.

The presence of such "lingual" cartilage has been asserted only in extant lampreys and hagfishes (26), but also suggested in euphaneropids (34) and fossil lampreys (35, 36). Hence, even if it is supported by indirect evidence and not by actual cartilage remains or imprints that future investigations may reveal, our reconstruction lends strong support to a vertebrate affinity of conodonts as stem cyclostomes or possibly as the most "primitive" stem gnathostomes (i.e., between lampreys and "ostracoderms") (Fig. 6). It also suggests that this cartilage associated with protractor and retractor muscles is a plesiomorphic condition of crown vertebrates (that is lost in gnathostomes) [a similar hypothesis is proposed by Janvier (37)]. Because at least some conodonts were predators or scavengers (8), this cartilage was not, as often suggested (36), a specialized feature associated with a parasitic feeding habit.

Methods

The specimens were scanned using PPC-SRμCT at the European Synchrotron Radiation Facility (ESRF) on the beamline ID19. Further details on the set-up are in the *SI Methods*. The volumes were reconstructed using a filtered backprojection algorithm (PyHST, ESRF), and the model was computed using both the commercially available Amira imaging software and the in-house software FoRM-IT, developed by C. Zollikofer (University of Zurich).

1. Janvier P (2007) *Major Transitions in Vertebrate Evolution*, eds. Anderson JS, Sues H-D (Indiana University Press, Bloomington), pp 57–121.
2. Turner S, et al. (2010) False teeth: Conodont-vertebrate phylogenetic relationships revisited. *Geodiversitas* 32:545–594.
3. Donoghue PCJ, Sansom IJ (2002) Origin and early evolution of vertebrate skeletonization. *Microsc Res Tech* 59:352–372.
4. Donoghue PCJ (1998) Growth and patterning in the conodont skeleton. *Philos Trans R Soc Lond B Biol Sci* 353:633–666.
5. Purnell MA, Donoghue PCJ (1997) Architecture and functional morphology of the skeletal apparatus of ozarkodinid conodonts. *Philos Trans R Soc Lond B Biol Sci* 352:1545–1564.
6. Purnell MA, Donoghue PCJ (1998) Skeletal architecture, homologies and taphonomy of ozarkodinid conodonts. *Palaeontology* 41:57–102.
7. Purnell MA, Von Bitter PH (1992) Blade-shaped conodont elements functioned as cutting teeth. *Nature* 359:629–630.
8. Purnell MA (1995) Microwear on conodont elements and macrophagy in the first vertebrates. *Nature* 374:798–800.
9. Purnell MA, Donoghue PCJ, Aldridge RJ (2000) Orientation and anatomical notation in conodonts. *J Paleontol* 74:113–122.
10. Briggs DEG, Clarkson ENK, Aldridge RJ (1983) The conodont animal. *Lethaia* 16:1–14.
11. Orchard MJ (2005) Multielement conodont apparatuses of Triassic Gondolelloidea. *Conodont Biology and Phylogeny: Interpreting the Fossil Record*, eds. Purnell MA, Donoghue PCJ, (Spec Pap Palaeontol), Vol 73, pp. 73–101.
12. Zhang H, Tong J, Zuo J (2005) Lower Triassic and carbon isotope in West Guangxi, Southwest China. *International Symposium on Triassic Chronostratigraphy and Biotic Recovery* (Albertiana, Vol 33, Part I: Program and Abstracts), pp. 103–104.
13. Galfetti T, et al. (2008) Evolution of Early Triassic outer platform paleoenvironments in the Nanpanjiang Basin (South China) and their significance for the biotic recovery. *Sed Geol* 204:36–60.
14. Tafforeau P, et al. (2006) Applications of X-ray synchrotron microtomography for non-destructive 3D studies of paleontological specimens. *Appl Phys. A* 83:195–202.
15. Orchard MJ, Rieber H (1999) Multielement *Neogondolella* (Conodonta, upper Permian–middle Triassic). *Boll Soc Paleontol Ital* 37:475–488.
16. Rieber H (1980) Ein Conodontencluster aus der Grenzbitumenzone (Mittlere Trias) des Monte San Giorgio. *Ann Naturhist Mus Wien* 83:265–274.
17. Ramovs A (1978) Mitteltriassische Conodonten-clusters in Slowenien, NW Jugoslawien. *Paläont Z* 52:129–137.
18. Huang J-Y, et al. (2010) Discovery of Middle Triassic conodont clusters from Luoping Fauna, Yunnan Province. *Earth Science—Journal of China University of Geosciences* 35:512–514.
19. Sweet WC (1988) *The Conodonta: Morphology, Taxonomy, Paleoecology and Evolutionary History of a Long-Extinct Animal Phylum. Oxford Monographs on Geology and Geophysics 10* (Clarendon Press, Oxford), p 212.
20. Mashkova TV (1972) *Ozarkodina steinhornensis* (Ziegler) apparatus, its conodonts and biozone. *Geologica et Palaeontologica* 1:81–90.
21. Nicoll RS, Rexroad CB (1987) Re-examination of Silurian conodont clusters from Northern Indiana. *Palaeobiology of Conodonts*, ed Aldridge RJ (Ellis Horwood Limited, Chichester, UK), pp 49–61.
22. Schmidt H (1934) Conodonten-Funde in ursprünglichem Zusammenhang. *Paläont Z* 16:105–135.
23. Hilliard RW, Potter IC, Macey DJ (1985) The dentition and feeding mechanism in adults of the Southern Hemisphere lamprey *Geotria australis* Gray. *Acta Zool* 66:159–170.
24. Koike T, Yamakita S, Kadota N (2004) A natural assemblage of *Ellisonia* sp. cf. *E. triassica* Müller (Conodonta) from the Permian-Triassic boundary in the Suzuka Mountains, Central Japan. *Paleontol Res* 8:241–253.
25. Nicoll RS (1977) Conodont apparatus in an Upper Devonian palaeoniscoid fish from the Canning Basin, Western Australia. *BMR J Aust Geol Geophys* 2:217–228.
26. Tolmacheva TY, Purnell MA (2002) Apparatus composition, growth, and survivorship of the Lower Ordovician conodont *Paracordylodus gracilis* Lindström, 1955. *Palaeontology* 45:209–228.
27. Donoghue PCJ, Forey PL, Aldridge RJ (2000) Conodont affinity and chordate phylogeny. *Biol Rev Camb Philos Soc* 75:191–251.
28. Krejsa RJ, Bringas PJ, Slavkin HC (1990) A neontological interpretation of conodont elements based on agnathan cyclostome tooth structure, function, and development. *Lethaia* 23:359–378.
29. Yalden DW (1985) Feeding mechanisms as evidence of cyclostome monophyly. *Zool J Linn Soc* 84:291–300.
30. Donoghue PCJ, Purnell MA (2005) Genome duplication, extinction and vertebrate evolution. *Trends Ecol Evol* 20:312–319.
31. Donoghue PCJ, Graham A, Kelsh RN (2008) The origin and evolution of the neural crest. *Bioessays* 30:530–541.
32. Donoghue PCJ, Purnell MA, Aldridge RJ, Zhang S (2008) The interrelationships of 'complex' conodonts (Vertebrata). *J Syst Palaeontol* 6:119–153.
33. Aldridge RJ, Purnell MA, Gabbott SE, Theron JN (1995) The apparatus architecture and function of *Promissum pulchrum* Kovacs-Endrody (Conodonta, Ordovician) and the prioniodontid plan. *Philos Trans R Soc Lond B Biol Sci* 347:275–291.
34. Janvier P, Arsenault M (2007) The anatomy of *Euphanerops longaevus* Woodward, 1900, an anaspid-like jawless vertebrate from the Upper Devonian of Miguasha, Quebec, Canada. *Geodiversitas* 29:143–216.
35. Gess RW, Coates MI, Rubidge BS (2006) A lamprey from the Devonian period of South Africa. *Nature* 443:981–984.
36. Bardack D, Zangerl R (1968) First fossil lamprey: A record from the Pennsylvanian of Illinois. *Science* 162:1265–1267.
37. Janvier P (1981) The phylogeny of the Craniata, with particular reference to the significance of fossil "agnathans." *J Vertebr Paleontol* 1:121–159.